Thermosensitive poly(N-vinylcaprolactam) as a transmission light regulator in smart windows

Renata L. Sala[a], Ricardo H. Gonçalves[a], Emerson R. Camargo[a,*], Edson R. Leite[a,b]

[a] Department of Chemistry, Federal University of São Carlos (UFSCar), Rod. Washington Luis km 235, São Carlos, SP 13565-905, Brazil
[b] Brazilian Nanotechnology National Laboratory (LNNano, CNPEM), Rua Giusepe Máximo Scalfaro 10000, Campinas, SP 13083-970, Brazil

ABSTRACT

Upcoming generation of smart windows requires simple design, fast stimulus response and cost-effective production. Aiming these features, we reported a new approach of switchable devices based on the thermosensitive polymer poly(N-vinylcaprolactam) (PNVCL) and facile assembly of the components (FTO layers and polymer). Its optical/color change from transparent to opaque is temperature-dependent and activated by induced Joule heating of conductive substrates. Therefore, the reported devices showed fast reversible response (less than 60 s) by small input power and adjustable opaqueness according to polymer concentration. In opposite to traditional electrochromic smart windows dependence of the kinetics charge-transfer reaction, the observed features are triggered by the thermodynamic mechanism of the reversible coil-globule transition from PNVCL suspension, which can lead to stable performance of the proposed device.

1. Introduction

Smart windows (SW) are one of the most promising green technologies for energy harvesting, which next generation breakthrough relies on climate adaptive buildings by the regulation of solar energy transmission. These devices are designed to reduce air conditioning costs through sunlight blocking in summer and improve light harvesting during winter. Their fundamental mechanism is based on the tunable optical transmittance of incorporated switchable devices, generally promoted as a response of an applied bias or changes in environmental conditions [1].

Traditionally, switchable devices employ electrochromic materials based on transition metal oxides, suspended particles or polymers dispersed in liquid crystals as active materials [2,3]. These SW are composed of multilayers of components, which color modulation is commonly achieved by oxidation/reduction processes and diffusion of ions activated by an external stimulus [4]. Then, some features as fast coloration/bleaching response to external voltage [5] and glare control can be obtained for electrochromic SW [6]. However, this type of device can be costly, require demanding steps for materials development and multilayers construction, which can also lead to reduced visible transmittance and limited modulation level [7–9]. Additionally, since they change their optical properties by switching between oxidized and reduced form [4], these electrochemical reactions can have a reduced performance overtime due to unwanted side reactions between the

electrolyte and active materials [10], as decomposition of electrolytes and efficiency reduction of charge transfer reaction between the electrolyte and active materials [11,12].

Another class of switchable devices is based on thermotropic materials as polymer blends [13], hydrogels [14,15], block copolymers [16] and core/shell structures [17–20], being also reported in the patent literature [18]. They present a temperature-induced switching behavior caused by phase transition or separation process, or even differences in refractive indices of SW components. When the switching threshold is reached by the increase of temperature, the thermotropic material undergoes a phase transition, forming scattering domains with dimensions comparable to the wavelength of the solar spectral range that reflect the incident solar radiation [18,19,21]. Some features found for these switchable devices are low cost of products, passively switching mechanism with solar heat, and diversity of smart windows size and shape [18].

Among these thermotropic materials, thermosensitive polymers have the ability to fine-tune their transparency in response to surrounding conditions, inasmuch as they are structure/color-sensitive to temperature [14,19] and exhibit a cloud point in water or other solvents [21]. Thermosensitive polymers have been synthesized based on many formulations of synthetic and natural hydrogels [21], which features are highlighted in many biological applications, such as drug delivery, biosensors [22], tissue engineering and biotechnology [21]. On the other hand, the application of these materials as stimuli-

sensitive materials in light-shielding switchable devices still remains little explored. The principle of thermosensitive polymers in switchable devices is their coil-globule transition in aqueous solution at specific temperature, called lower critical solution temperature (LCST), induced by solar energy or sensing environmental temperature changes [23]. Below this temperature, polymer chains are soluble in water by predominant hydrophilic forces and the medium is transparent [24,25]. However, when the system is heated above the LCST, intra- and interpolymer interactions predominate, resulting in a homogeneous opaque agglomerate state promoted by hydrophobic interactions. The great advantage of employing this class of thermosensitive polymers in SW is the longtime stability assured by entropic effect, high transparency in the clear state with low haze, outstanding switching performance and reversibility and steep switching gradient [21].

Polymer chain size and structure, as well as the type of solvent, affect the swelling/deswelling kinetic of thermosensitive systems. For instance, Wang et al. [26] showed poly(N-isopropylacrylamide) (PNIPAm) microgels in the presence of glycerol had lower thermosensitive response speed, since the presence of other molecules in the medium alters the hydrophilic and hydrophobic balance of the system. PNIPAm has been used as thermotropic component of SW [26,27] to respond to sunlight irradiation [19], change their optical properties by applying a high-frequency AC current [28], as well as a sweating component to passively cool buildings [29]. Nevertheless, PNIPAm is always combined with other materials to have its critical temperature adjusted to be suited for switchable devices [2], increasing the cost and hindering the development of SW.

Another thermosensitive polymer that has gained prominence is the poly(N-vinylcaprolactam) (PNVCL, $(C_8H_{13}NO)_n$). Although its broad application has been in the biomaterials field [30], PNVCL is a promising material for SW. The main difference between PNVCL and PNIPAm is regarding their phase transition in water. PNVCL exhibits a type I critical miscibility in water, which LCST decreases and shifts towards lower polymer concentration with increased molecular weight. On the other hand, PNIPAm represents a type 2, which LCST is independent of the molecular weight and is hardly affected by environmental conditions [31], being usually modified by the presence of co-monomers. In this way, the LCST of PNVCL can be shifted to lower or higher temperatures just by changing chemical composition as the addition of salts [32], different solvents, copolymers [33], presence of surfactants [34] or even changing polymer structure or its molecular mass [30,35]. The possibility of having versatile LCST values allow the application of PNVCL for several environmental temperatures.

Here, we demonstrate an innovative application by using PNVCL as active material in SW devices, taking advantage of its capacity to modify the device transmittance according to the temperature, which can be achieved by induced heating of conductive substrates. Thereby, the color/optical transmittance of the smart windows can be changed anytime, without the need to reach a switching threshold in response to intense solar heating, as found in many passively switching systems based on thermotropic materials [19,36].

Concurrently, we were able to propose a singular approach to produce switchable devices composed by a facile assembly of the components (transparent conductive substrates and active material) and operation system supported by an applied voltage. In comparison to other switchable devices based on thermosensitive polymers [15,27,28,37], we designed a versatile and highly efficient device system dependent of a heating stimulus induced by small input power, requiring less energy consumption and just a thin layer of PNVCL suspension to undergo a reversible process of color and optical properties.

2. Materials and methods

2.1. Materials

N-vinylcaprolactam monomer (NVCL, 415464, Sigma-Aldrich ≥

98%, USA) and dimethyl sulfoxide (p.a., ACS reagent, Synth, Brazil) were used as received. The 2,2′-azobis(2-methylpropionitrile) initiator (AIBN, DuPont, Brazil) was previously recrystallized in methanol. Switchable devices were constructed with transparent and conductive substrates made of fluorine-doped tin oxide (FTO) coated glass with a resistivity of 10 Ω/sq. and thickness of 1 mm (TCO10-10, Solaronix, Switzerland).

2.2. Synthesis and characterization of PNVCL

For the synthesis of PNVCL, NVCL monomer crystals were dispersed in dimethyl sulfoxide (15 wt%) and heated until 70 °C under N_2 atmosphere. Then, 2% w/w of AIBN initiator was dropwise added to the system and the reaction proceeded for 4 h. The PNVCL with Mn = 12.9 kDa was purified after being centrifuged and washed in hot deionized water for four times and dried at 60 °C in an lab oven with forced air circulation.

2.3. Smart windows building

Smart windows were built with two FTO substrates as a heating element and dynamical control of the temperature by bias applied. They were cut in square shapes with 2.5 cm of length and sealed with double-sided adhesive tape (VHB, 3 M Scotch® clear mounting tape 19 mm x 2 m, Brazil) and conductive liquid silver contacts (16062, PELCO® conductive silver paint, Ted Pella, USA), keeping the gap between the substrates of approximately 375 μm. Then, the device was filled with an aqueous solution with 1 and 5 wt% of PNVCL (Fig. 1) by using a syringe with a needle of 26 G, well-sealed with quick setting epoxy to avoid any leakage and drying out, and connected to a current voltage power supply unit (Hp E3611A power supply 0–020 VDC 1.5 A / 0–35 VDC 85 A 35 W).

2.4. Characterization

Liquid-state NMR experiments were performed on a Bruker Avance III spectrometer operating at a magnetic field of 9.4 T Oxford, with the related frequency of 400 MHz for the hydrogen-1 nucleus. Analyzes were performed with a tunable probe for a wide range of frequencies (40–160 MHz) and with 10 mm diameter tubes. PNVCL and its monomer were dispersed in 2.5 mL of water and chloroform, respectively, and D_2O and $CDCl_3$ were used as external standard. ^{13}C spectra were obtained qualitatively at room temperature in the fully coupled mode using NOE (Nuclear Overhauser Effect) transfer with an acquisition time of 0.55 s and relaxation time of 0.1 s.
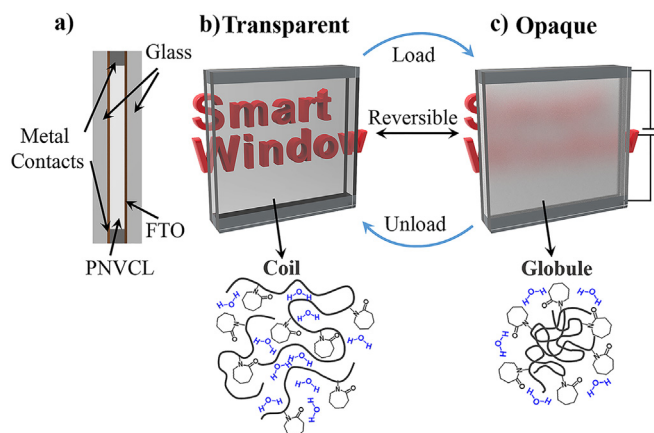
Fig. 1. Illustrative diagram of the smart window. (a) Assembly of two FTO substrates with a small gap filled up with PNVCL suspension. (b) Representative switch between transparent and opaque SW (c) during the coil-globule transition when applied a power supply.

The transmittance of PNVCL aqueous solution (1 and 5 wt%) measured at the wavelength range (200–800 nm) from 25° to 35°C was analyzed in a Multi-Spec-1501 UV–vis Spectrophotometer Shimadzu with a TCC-240A thermoelectrically temperature controlled cell holder, to investigate the lower critical solution temperature of the materials. The temperature was allowed to stabilize for 5 min before the measurement of the transmittance. The thermoresponse of PNVCL suspensions induced by bias supply was also analyzed by in situ UV–vis spectroscopy, by measuring the transmittance in triplicate of switchable devices filled with PNVCL suspensions (1 and 5 wt%) against an applied voltage at continuous current, allowed to stabilize for 5 min before the measurement of the transmittance. The wavelength range was investigated between 350 and 800 nm due to characteristic absorption band of FTO coated glasses below 350 nm. The device surface temperature was measured by infrared digital thermometer (G-Tech, Brazil).

Solar light transmittance of SW with 1 or 5 wt% of PNVCL was investigated using an artificial source in the range of 350–1100 nm. For this analysis, we employed the Oriel Quantum Efficiency Measurement System (Newport) model 74125, with 300-watt xenon arc lamp. The samples were allowed to stabilize for 5 min in each applied voltage before the measurement of the transmittance.

Dynamic Light Scattering (DLS) analyses of the hydrodynamic diameter (D_h) of PNVCL dispersed in deionized water (1 wt%) as a function of the temperature was carried out on Zetasizer Nano ZS (Malvern) at an angle of 173°, with a He−Ne 4.0 mW power laser operating at 633 nm. The samples were allowed to stabilize for 5 min in each temperature before triplicate measurements of D_h.

Micrographs of the globule-coil transition of PNVCL suspension (1 wt%) on a cover slip were taken from the same area of the sample using a hot-stage microscopy (Modular Polarization Microscope Leica DM2500 P coupled with a Linkam T95-PE device) with 200 × magnification. For this experiment, 25 μL of PNVCL suspension was heated from 25° to 40°C at a heating rate of 5 °C/min. This heating rate was chosen to guarantee that the sample would not dry during the experiments. The cooling process was investigated during natural cooling of the sample up to room temperature.

3. Results and discussion

N-vinylcaprolactam monomer has an amphiphilic character by the presence of the amide ring group (caprolactam) bound to a hydrophobic vinyl group. From this group, it is possible to carry out the free radical polymerization in the presence of the AIBN initiator at 70 °C. The resulting PNVCL is water-soluble and when dispersed in an aqueous solution and heated up to its characteristic LCST, a phase transition occurs from solvated polymer chains to a globule state. By ^{13}C NMR spectra at Fig. 2, pure phase of PNVCL was obtained by the absence of methylene groups at 131.4 and 97.4 ppm from the precursor monomer. ^{13}C chemical shift values for PNVCL and monomer and their corresponding functional groups are described as: 22.3 ppm (C6), 28, 3 ppm (C5), 29.3 ppm (C4), 33.9 ppm (C1), 36.8 ppm (C7), 42.4 ppm (C3), 47.4 ppm (C2), 178.4 ppm (C8), 97.4 ppm (C1') and 131.4 ppm (C2').

Superior SW should exhibit high transmittance in a full-range visible spectrum and be able to self-regulate, which is a hard task to be achieved when dealing with electrochromic or multilayers devices due to their reduced transparency in some range of the solar spectra [38,39]. In order to demonstrate how PNVCL as active material could overcome those hindrances, its ability to regulate the light transmission was initially investigated by ultraviolet–visible (UV–vis) spectrophotometry using typical quartz cuvette. Differences in turbidity (from transparent to opaque) of PNVCL suspensions were measured by the observation of the cloud point (first change of the scattered light) when these systems were heated from 25° to 35°C. Fig. 3a shows transmittance spectra of a diluted aqueous suspension of PNVCL (1%) collected in a wide range of UV and visible light at different temperatures. At
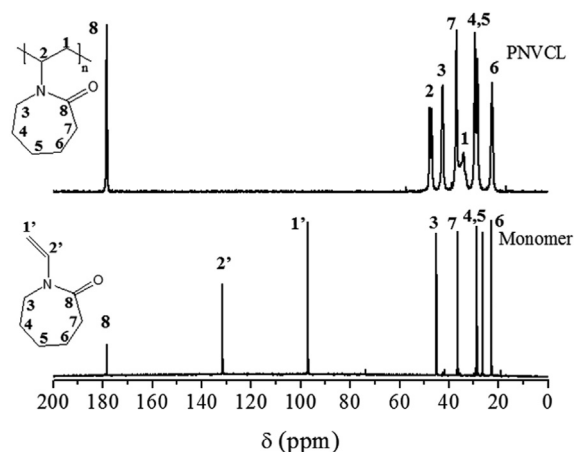

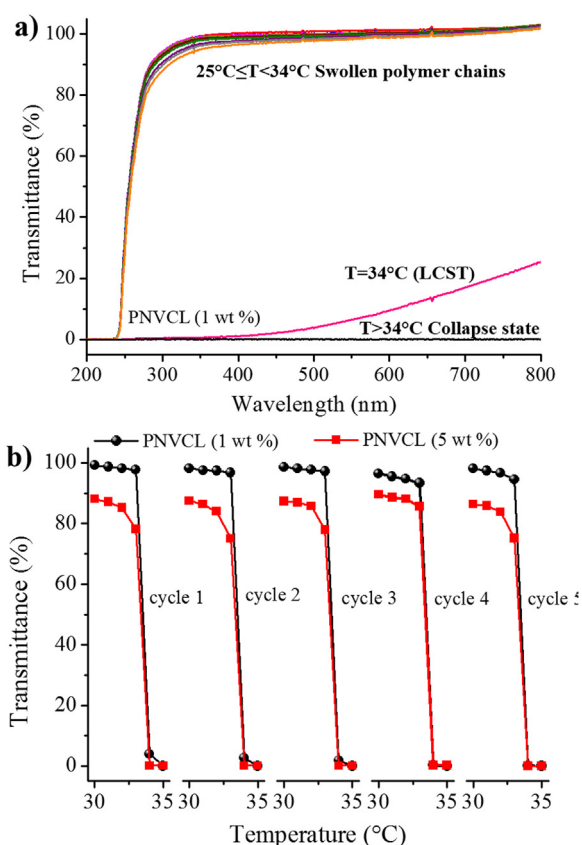**Fig. 2.** ^{13}C NMR spectra of PNVCL and its monomer in D_2O and $CDCl_3$, respectively.

Fig. 3. (a) UV–vis transmittance spectra of a diluted suspension of PNVCL (1 wt %) from 25 °C to 35 °C. (b)Temperature-dependent transmittance at λ = 500 nm of PNVCL suspensions (1 and 5 wt%) over 5 independent sequential cycles from 30 °C to 35 °C.

temperatures below 34 °C, which value could be characterized as the LCST for the PNVCL, the system is transparent due to polymer solvation in water. On the other hand, it becomes opaque during the hydrophilic/hydrophobic phase transition that occurs at 34 °C, blocking the passage of light at higher temperatures. In fact, this transition is better observed plotting the transmittance of PNVCL suspensions at fixed wavelength (λ = 500 nm) against temperature (Fig. 3b). Each sample was heated from 30° to 35°C, range where the LCST is seen, and cooled down at room temperature before beginning a new heating cycle, which was repeated five times.

Transmittance profile of each cycle was identical to the previous, suggesting an excellent reproducibility. However, while diluted PNVCL suspension (1%) exhibited a transmittance of around 100% at temperatures below the LCST, its concentrated suspension (5%) had a transmittance of 88%. This dependence of transmittance on the amount of dissolved polymer is in agreement with the Lambert-Beer law, which suggests an easy way to tune the transparency of the SW below LCST, by simply adjusting the concentration of the active material or optimizing geometrical characteristics of SW. Despite this difference in the initial transmittance of suspensions according to PNVCL concentration, both systems exhibited the same LCST. Additionally, no polymer precipitation was observed during heating and cooling experiments. Since the transmittance regulation of thermosensitive polymers takes place according to the coil-globule transition with temperature, it is possible the occurrence of phase separation depending of polymer concentration or molecular weight. In that case, the phase separation can be prevented by the use of surfactants, as demonstrated by McPhee et al. [40], ensuring the consistency and applicability of thermosensitive polymers in SW.

Once the temperature-induced phase transition was identified at 34 °C for PNVCL suspensions, it is possible to study the variation of SW temperature induced by a power supply. With the passage of electric current through FTO substrates, heat is generated by Joule effect, inducing the increase of PNVCL temperature and its coil-globule transition. Fig. 4 shows the transmittance at $\lambda = 500$ nm against an applied voltage of SW filled with 1% (Fig. 4a) and 5% (Fig. 4b) of PNVCL suspensions, where error bars represent the variability of triplicate data. The variability among data was very small for most temperatures, resulting in errors bars with size that did not exceed the size of graph points. SW spectra from 350 to 800 nm with the applied voltage can be
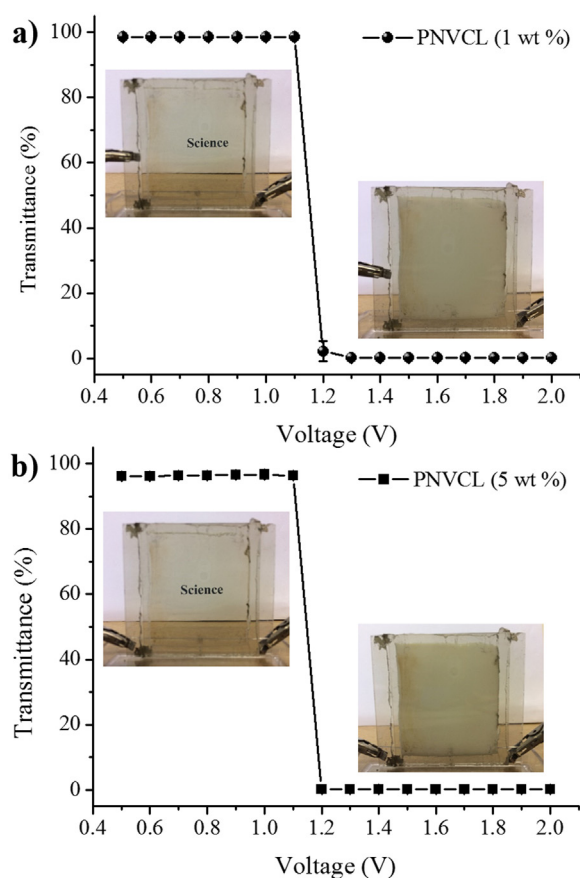
seen at Fig. S1 in Supplementary Material. These two PNVCL suspensions show similar transmittance values since the optical path through the thinner layer of polymer inside the device (375 µm) was much shorter than in a quartz cuvette in the previous experiments. Both devices presented a transmittance change at the same voltage (1.2 V), which is related to the required energy to heat the system and induce the phase transition of PNVCL suspensions, independently of polymer concentration. Additionally, both PNVCL suspensions fully suppressed the image behind the SW in Fig. 4. Compared to other electrochromic devices [2,9,27], we reported a smart window with a thermosensitive active polymer with transparency higher than 96% before coil-globule transition, and a high modulation luminous transmittance with an applied bias.

The conductive substrate also influences the SW performance. In this study, commercial FTO substrates with specific conductive layer (10 Ω/sq.) were used as a conductive substrate due to its transparency, thermal and chemical stability, as well as stable resistivity with temperature [29–31]. Changing the substrate properties will influence the smart windows performance and energy consumption. Fischer et al. [28] demonstrated that increasing the thickness of Sn-doped indium oxide layers in light filters reduced the switching time of thermotropic materials, as well as the required power for the process. Although better properties can be obtained by using thicker SW, changing the thickness of the conductive substrate also implies in a higher cost of the substrate, and affects the light transmittance of the device. SW performance can be seen in Fig. 5, and according to the PNVCL transition temperature of 34 °C, the current, voltage and power required for the switching process take place is 0.16 A, 1.2 V and 0.19 W, respectively. Then, the proposed smart window needed an input power of 0.03 W/cm^2 to switch the system from transparent to opaque, demanding less energy consumption for its operation and greater performance than switchable devices that employed thermosensitive polymers as PNIPAm and
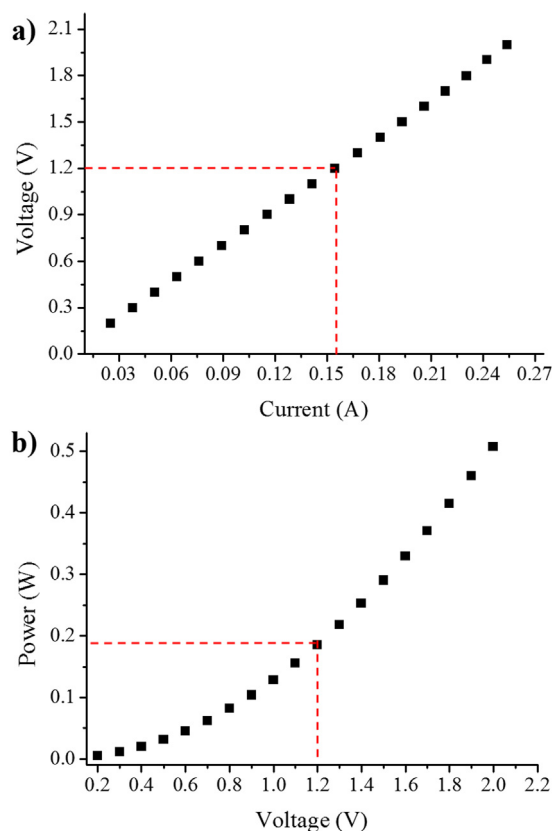

Fig. 4. Smart windows transmittance (%) at $\lambda = 500$ nm versus applied voltage for (a) PNVCL (1 wt%) and (b) PNVCL (5 wt%).%). Error bars represent the variability of triplicate data.
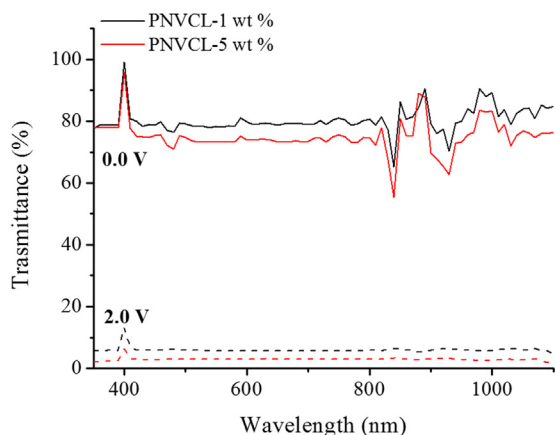

Fig. 5. (a) Variation of voltage x current, (b) energy consumption (power x voltage) for the smart windows.

Fig. 6. Solar light transmittance spectra of smart windows filled with PNVCL 1 or 5 wt% at room temperature (when no bias was applied, 0.0 V) and when heated by applying 2.0 V.

hydroxypropyl methyl cellulose [27,28,37,41].

Additionally, high modulation ability to solar light transmission was attained to these SW. Fig. 6 shows the transmittance versus wavelength of the device filled with PNVCL 1 or 5% when heated by applying a continuous supply of 2.0 V or 0.0 V (room temperature). A transmittance between 60% and 90% was observed when no voltage was applied, which switched to less than 5% when the device was heated by applying 2.0 V, demonstrating high transmission modulation ability in the wavelength range. Some reduction of transmittance above 840 nm when no voltage was applied is related to FTO substrate absorption in the near-infrared region.

Another desirable feature for SW is a quick response to a specific stimulus. Aiming to measure the time necessary for the PNVCL to undergo a phase transition by induced heating from a power supply, a fixed voltage was applied to the device and its transmittance evaluated at $\lambda = 500$ nm over time. Fig. 7a shows the transition from transparent to opaque states happens in 60 s of continuous supply of 2.0 V, demonstrating the efficiency of the polymer to respond to an induced heating generated by the applied bias on FTO substrates. In order to investigate the cooling process, the power source was stopped and the hot device (35 °C) kept cooling down naturally to room temperature, requiring no more than 150 s to return to its transparent swollen state (Fig. 7b). The response times needed for the smart window to heat and cool down were smaller compared to reported devices that employed thermosensitive materials as active component. For instance, PNIPAm bulk hydrogels have shown to take several minutes (up to 40 min) to

undergo the phase transition during heating and cooling processes [28], while PNIPAm microgels required 250 s for each process [26], and hydroxypropyl methyl cellulose materials required 360 s for the cooling process [37]. Additionally, a short switching time for the device suggests that the time expended by this SW based on PNVCL suspensions to regulate the transmission light is also inherently dependent of the heat capacity of support material.

PNVCL is considered a non-degradable polymer and its coil-globule transition is associated with thermodynamic changes of the system. These combined features could lead to switchable devices based on PNVCL with long lifespan, compared to traditional kinetic-based devices that involve chemical reactions [9]. The cycle stability of PNVCL suspensions in the process of changing from transparent to opaque with an applied voltage is shown in Fig. 7c. PNVCL suspensions showed high ability to modulate the light transmission over 50 repeated cycles, as well as reversible opaque-transparent transitions by applying 2.0 V or turning it off, without any significant variation. In this way, the performance of SW was stable during the measurements, without the presence of polymer phase separation.

Additionally, the structural changes of the thermotropic transition of PNVCL suspension (1 wt%) was investigated by dynamic light scattering (DLS) in the temperature range from 25° to 40°C. Fig. 8 shows the average hydrodynamic diameter (D_h) of PNVCL suspension increased when the coil-globule transition takes place, and in the Fig. S2 (Supplementary Material), it is possible to observe the size distribution by number of PNVCL suspension at 25 °C, 34 °C and 40 °C. Below the LCST, D_h is ~ 10 nm, suggesting that the polymers are present as free polymer chains. Since the PNVCL was synthesized in bulk, when the system is heated and reaches the LCST, polymer chains aggregate by hydrophobic association forming large particles (~ 5000 nm). This increase of D_h with temperature has already been reported by previous studies [42–46], and the found threshold temperature for the polymer macromolecular aggregation was consistent with the one measured by UV − visible spectroscopy in this study. When thermosensitive polymers are synthesized as microgel, the behavior is opposite and the particles undergo a volume phase transition and their D_h reduce above the LCST, due to their shrinking according to the transition from swollen to collapsed state [47–50].

At temperatures above LCST, thermosensitive polymeric chains are aggregate due to predominant physical hydrophobic interactions that exceed swelling forces. This agglomerated state is well-evidenced in Fig. 9, which represents a sequence of micrographs taken from the same area of the sample and illustrates the PNVCL morphological changes over time, during heating and cooling processes.

According to the images obtained in Fig. 9, during the heating
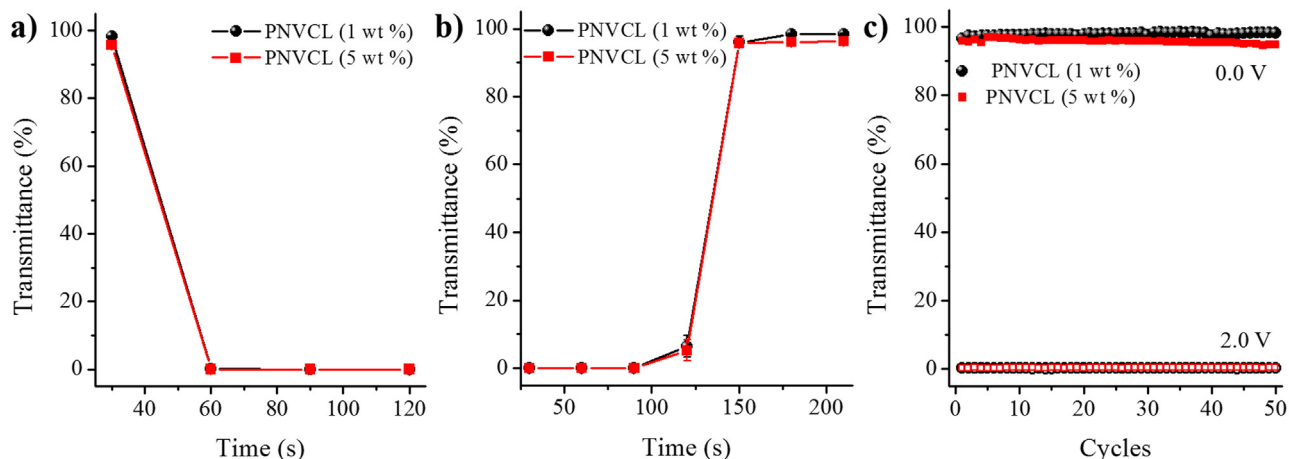
Fig. 7. a) Smart windows transmittance (%) at $\lambda = 500$ nm with time by applying 2.0 V or b) cooling with no bias applied, and c) during 50 independent sequential cycles. Error bars represent the variability of triplicate data.
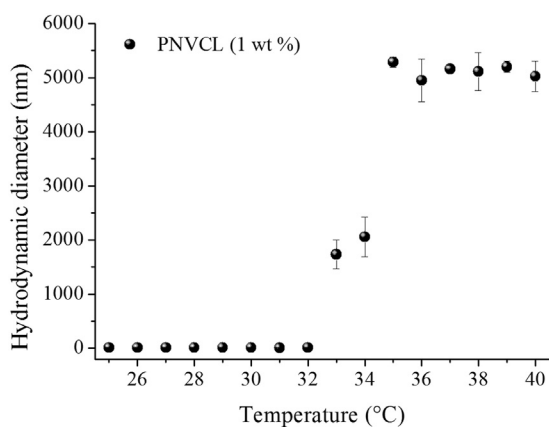
Fig. 8. Variation of the average hydrodynamic diameter of PNVCL suspension (1 wt%) with temperature. Error bars represent the variability of triplicate data.

process polymer chains start to self-aggregate into small polydispersed microparticles (31 °C). With continuing heating and reaching of the LCST, those microparticles grow ($\sim$ 4 μm at 34 °C) and keep increasing in size by coalescence with some neighboring microparticles ($\sim$ 6 μm at 36 °C and $\sim$ 12 μm at 40 °C). It is important to highlight that some size differences between optical microscopy and DLS measurements can be related to the inability of DLS analysis to detect particles with hydrodynamic diameter higher than 10 μm, as well as small degree of water evaporation during optical microscopy experiment could induce the coalesce between neighboring globules. Additionally, these microparticles probably grow until a limited size, keeping stable over the analyzed time. Such behavior is evidenced by a stable D_h of $\sim$ 5 μm of the structures above the LCST by DLS, which exist as the predominant population in the distribution of globules by number at Fig. S2. During cooling, the globules get bigger average size, i.e. $\sim$ 17 μm at 39 °C, $\sim$ 22 μm at 36 °C, $\sim$ 29 μm at 34 °C and $\sim$ 34 μm at 31 °C, especially due to the swelling of microparticles and coalescence with neighboring globules. It is interesting to note that the microparticles size and morphology change differently during the coil-to-globule and the globule-to-coil transitions. During the heating process, polymer chains collapsed into small structures, following by a growth probably due to the coalescence of globules formed by contracted chains, and agglomeration of interpenetrating chains [51]. On the other hand, the globules persisted with similar or bigger sizes during the cooling process, until

they become completed swollen again at 25 °C, being no longer possible to be observed by optical microscopy. Wang et al. [52] described those previous structures as molten globules, which represented an intermediated state between the coil and collapsed states. These molten globules could be related to the difficulty of swelling intrachain and interchain structures present in the globule state, which prevented them to swell directly upon cooling [52,53]. Additionally, Cheng et al. [53] described the existence of remaining intersegmental hydrogen bonds between polymer hydrophilic groups and water molecules inside the collapsed state, which keep the system interconnected like a gel, allowing it to swell (as observed during the cooling step), but delaying chains dissociation. In this way, although the coil is the thermodynamic state at lower temperatures during the cooling, there is a kinetic factor delaying the swollen process related to these intermediate globules. It's worth highlighting that both studies [52,53] reported those results based on light scattering analysis, while we could monitor the coil-globule transition by in situ optical microscopy.

4. Conclusions

We presented a novel approach of smart switchable devices formed by a thermosensitive PNVCL suspension heated by FTO conductive substrates powered by electric supply. These SW bring many distinct characteristics, as a reversible transition from a highly transparent state to opaqueness that can be finely adjusted either by modifying the chemical nature of the thermosensitive PNVCL or by optimizing the geometrical characteristics of SW. When compared to traditional SW, our device exhibits a fast response to heating stimulus induced by an applied bias and requires a notoriously small amount of power consumption. Therefore, this study provides a promising avenue toward the construction of high-performing temperature sensitive smart windows, advanced temperature/solar sensors and displays by using non-toxic materials in a system that can be passively activated by solar heating or by applying an electrical bias.

Acknowledgment
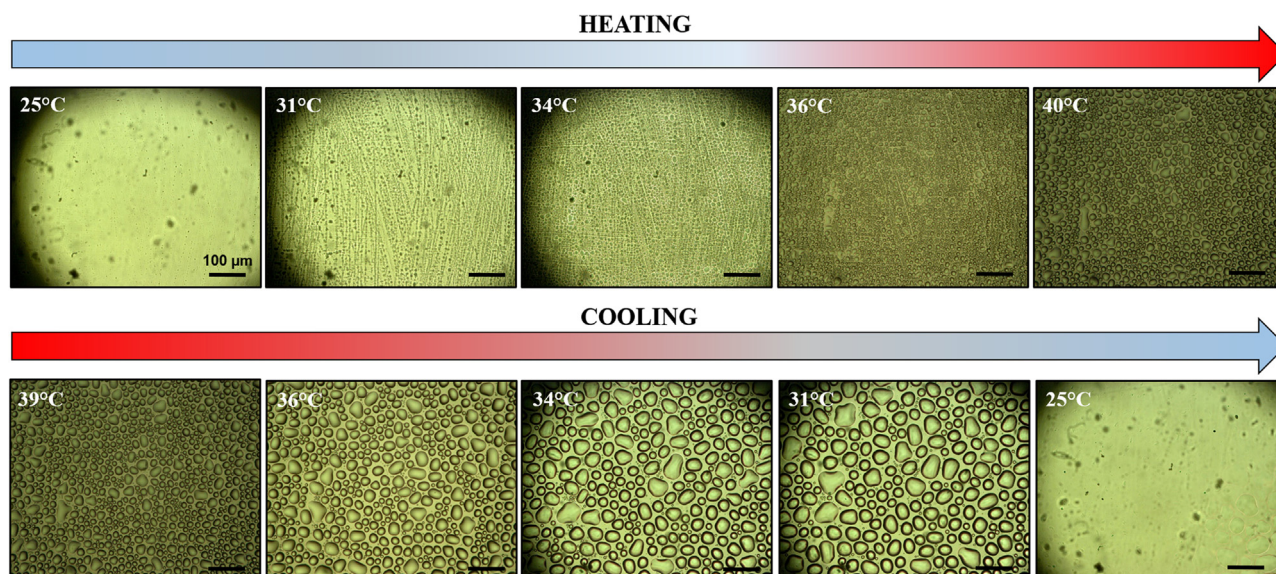
Fig. 9. Optical microscopy images of PNVCL solution (1 wt%) during heating and cooling processes.

Appendix A. Supplementary material

Supplementary data associated with this article can be found in the online version at http://dx.doi.org/10.1016/j.solmat.2018.06.037.

References

[1] W. Weng, T. Higuchi, M. Suzuki, T. Fukuoka, T. Shimomura, M. Ono, L. Radhakrishnan, H. Wang, N. Suzuki, H. Oveisi, Y. Yamauchi, A high-speed passive-matrix electrochromic display using a mesoporous TiO_2 electrode with vertical porosity, Angew. Chem. 122 (2010) 4048–4051.

[2] F. Chen, Y. Ren, J. Guo, F. Yan, Thermo- and electro-dual responsive poly(ionic liquid) electrolyte based smart windows, Chem. Commun. (2017).

[3] D. Jung, W. Choi, J.-Y. Park, K.B. Kim, N. Lee, Y. Seo, H.S. Kim, N.K. Kong, Inorganic gel and liquid crystal based smart window using silica sol-gel process, Sol. Energy Mater. Sol. Cells 159 (2017) 488–495.

[4] R. Baetens, B.P. Jelle, A. Gustavsen, Properties, requirements and possibilities of smart windows for dynamic daylight and solar energy control in buildings: a state-of-the-art review, Sol. Energy Mater. Sol. Cells 94 (2010) 87–105.

[5] C.-C. Wu, J.-C. Liou, C.-C. Diao, Self-powered smart window controlled by a high open-circuit voltage InGaN/GaN multiple quantum well solar cell, Chem. Commun. 51 (2015) 12625–12628.

[6] S.D. Rezaei, S. Shannigrahi, S. Ramakrishna, A review of conventional, advanced, and smart glazing technologies and materials for improving indoor environment, Sol. Energy Mater. Sol. Cells 159 (2017) 26–51.

[7] S. Bogati, A. Georg, W. Graf, Photoelectrochromic devices based on sputtered WO3 and TiO2 films, Sol. Energy Mater. Sol. Cells 163 (2017) 170–177.

[8] Z. Chen, C. Cao, S. Chen, H. Luo, Y. Gao, Crystallised mesoporous TiO2(A)-VO2(M/R) nanocomposite films with self-cleaning and excellent thermochromic properties, J. Mater. Chem. A 2 (2014) 11874–11884.

[9] W. Dong, Y. Lv, L. Xiao, Y. Fan, N. Zhang, X. Liu, Bifunctional MoO_3–WO_3/Ag/MoO_3–WO_3 films for efficient ITO–free electrochromic devices, ACS Appl. Mater. Interfaces 8 (2016) 33842–33847.

[10] J. Wang, L. Zhang, L. Yu, Z. Jiao, H. Xie, X.W. Lou, X. Wei Sun, A bi-functional device for self-powered electrochromic window and self-rechargeable transparent battery applications, Nat. Commun. 5 (2014) 4921.

[11] L. Xia, L. Yu, D. Hu, G.Z. Chen, Electrolytes for electrochemical energy storage, Mater. Chem. Front. 1 (2017) 584–618.

[12] K. Hu, A.D. Blair, E.J. Piechota, P.A. Schauer, R.N. Sampaio, F.G.L. Parlane, G.J. Meyer, C.P. Berlinguette, Kinetic pathway for interfacial electron transfer from a semiconductor to a molecule, Nat. Chem. 8 (2016) 853.

[13] A. Raicu, H.R. Wilson, P. Nitz, W. Platzer, V. Wittwer, E. Jahns, Facade systems with variable solar control using thermotropic polymer blends, Sol. Energy 72 (2002) 31–42.

[14] Y.-S. Yang, Y. Zhou, F.B. Yin Chiang, Y. Long, Temperature-responsive hydroxypropylcellulose based thermochromic material and its smart window application, RSC Adv. 6 (2016) 61449–61453.

[15] Y. Zhou, Y. Cai, X. Hu, Y. Long, Temperature-responsive hydrogel with ultra-large solar modulation and high luminous transmission for "smart window" applications, J. Mater. Chem. A 2 (2014) 13550–13555.

[16] X. Gong, J. Li, S. Chen, W. Wen, Copolymer solution-based "smart window", Appl. Phys. Lett. 95 (2009) 251907.

[17] O. Muehling, A. Seeboth, T. Haeusler, R. Ruhmann, E. Potechius, R. Vetter, Variable solar control using thermotropic core/shell particles, Sol. Energy Mater. Sol. Cells 93 (2009) 1510–1517.

[18] A. Seeboth, R. Ruhmann, O. Mühling, Thermotropic and thermochromic polymer based materials for adaptive solar control, Materials 3 (2010) 5143.

[19] D. Kim, E. Lee, H.S. Lee, J. Yoon, Energy efficient glazing for adaptive solar control fabricated with photothermotropic hydrogels containing graphene oxide, Sci. Rep. 5 (2015) 7646.

[20] A. Seeboth, D. Lötzsch, R. Ruhmann, O. Muehling, Thermochromic polymers—function by design, Chem. Rev. 114 (2014) 3037–3068.

[21] K. Resch, G.M. Wallner, Thermotropic layers for flat-plate collectors—a review of various concepts for overheating protection with polymeric materials, Sol. Energy Mater. Sol. Cells 93 (2009) 119–128.

[22] O. Sedláček, P. Černoch, J. Kučka, R. Konefal, P. Štěpánek, M. Vetřík, T.P. Lodge, M. Hrubý, Thermoresponsive polymers for nuclear medicine: which polymer is the best? Langmuir 32 (2016) 6115–6122.

[23] H. Watanabe, Intelligent window using a hydrogel layer for energy efficiency, Sol. Energy Mater. Sol. Cells 54 (1998) 203–211.

[24] M. Patenaude, T. Hoare, Injectable, degradable thermoresponsive poly(N-isopropylacrylamide) hydrogels, ACS Macro Lett. 1 (2012) 409–413.

[25] G. Charlet, R. Ducasse, G. Delmas, Thermodynamic properties of polyolefin solutions at high temperature: 2. Lower critical solubility temperatures for polybutene-1, polypentene-1 and poly(4-methylpentene-1) in hydrocarbon solvents and determination of the polymer-solvent interaction parameter for PB1 and one ethylene-propylene copolymer, Polymer 22 (1981) 1190–1198.

[26] M. Wang, Y. Gao, C. Cao, K. Chen, Y. Wen, D. Fang, L. Li, X. Guo, Binary solvent colloids of thermosensitive poly(N-isopropylacrylamide) microgel for smart windows, Ind. Eng. Chem. Res. 53 (2014) 18462–18472.

[27] Y. Zhou, M. Layani, F.Y.C. Boey, I. Sokolov, S. Magdassi, Y. Long, Electro-thermochromic devices composed of self-assembled transparent electrodes and hydrogels, Adv. Mater. Technol. 1 (2016) (1600069-n/a).

[28] T. Gyenes, A. Szilágyi, T. Lohonyai, M. Zrínyi, Electrically adjustable thermotropic windows based on polymer gels, Polym. Adv. Technol. 14 (2003) 757–762.

[29] A.C.C. Rotzetter, C.M. Schumacher, S.B. Bubenhofer, R.N. Grass, L.C. Gerber, M. Zeltner, W.J. Stark, Thermoresponsive polymer induced sweating surfaces as an efficient way to passively cool buildings, Adv. Mater. 24 (2012) 5352–5356.

[30] R.L. Sala, M.Y. Kwon, M. Kim, S.E. Gullbrand, E.A. Henning, R.L. Mauck, E.R. Camargo, J.A. Burdick, Thermosensitive poly(N-vinylcaprolactam) injectable hydrogels for cartilage tissue engineering, Tissue Eng. Part A (2017).

[31] J. Ramos, A. Imaz, J. Forcada, Temperature-sensitive nanogels: poly(n-vinylcaprolactam) versus poly(N-isopropylacrylamide), Polym. Chem. 3 (2012) 852–856.

[32] Y. Maeda, T. Nakamura, I. Ikeda, Hydration and phase behavior of poly(N-vinylcaprolactam) and poly(N-vinylpyrrolidone) in water, Macromolecules 35 (2002) 217–222.

[33] I. Popescu, A.I. Prisacaru, D.M. Suflet, G. Fundueanu, Thermo- and pH-sensitivity of poly(N-vinylcaprolactam-co-maleic acid) in aqueous solution, Polym. Bull. 71 (2014) 2863–2880.

[34] S. Peng, C. Wu, Surfactant effect on pH and temperature sensitivities of poly(N-vinylcaprolactam-co-sodium acrylate) microgels, Macromolecules 34 (2001) 568–571.

[35] S.F. Medeiros, J.C.S. Barboza, M.I. Ré, R. Giudici, A.M. Santos, Solution polymerization of N-vinylcaprolactam in 1,4-dioxane. Kinetic dependence on temperature, monomer, and initiator concentrations, J. Appl. Polym. Sci. 118 (2010) 229–240.

[36] C.M. Lampert, Chromogenic smart materials, Mater. Today 7 (2004) 28–35.

[37] S. Kiruthika, G.U. Kulkarni, Energy efficient hydrogel based smart windows with low cost transparent conducting electrodes, Sol. Energy Mater. Sol. Cells 163 (2017) 231–236.

[38] B. Robert, F. Manrico, V. Nastasja, Z. Kamil, S. Eliza, R. Lachlan, M. Peter, E. Drew, Effect of oxidant on the performance of conductive polymer films prepared by vacuum vapor phase polymerization for smart window applications, Smart Mater. Struct. 24 (2015) 035016.

[39] M.-H. Yeh, L. Lin, P.-K. Yang, Z.L. Wang, Motion-driven electrochromic reactions for self-powered smart window system, ACS Nano 9 (2015) 4757–4765.

[40] W. McPhee, K.C. Tam, R. Pelton, Poly(N-isopropylacrylamide) latices prepared with sodium dodecyl sulfate, J. Colloid Interface Sci. 156 (1993) 24–30.

[41] T. Fischer, R. Lange, A. Seebot, Hybrid solar and electrically controlled transmission of light filters, Sol. Energy Mater. Sol. Cells 64 (2000) 321–331.

[42] L. Etchenausia, A.M. Rodrigues, S. Harrisson, E. Deniau Lejeune, M. Save, RAFT copolymerization of vinyl acetate and N-vinylcaprolactam: kinetics, Control, copolymer composition, and thermoresponsive self-assembly, Macromolecules 49 (2016) 6799–6809.

[43] L. Etchenausia, A. Khoukh, E. Deniau Lejeune, M. Save, RAFT/MADIX emulsion copolymerization of vinyl acetate and N-vinylcaprolactam: towards waterborne physically crosslinked thermoresponsive particles, Polym. Chem. 8 (2017) 2244–2256.

[44] E.E. Makhaeva, H. Tenhu, A.R. Khokhlov, Behaviour of poly(N-vinylcaprolactam) macromolecules in the presence of organic compounds in aqueous solution, Polymer 41 (2000) 9139–9145.

[45] E.E. Makhaeva, H. Tenhu, A.R. Khokhlov, Behavior of poly(N-vinylcaprolactam-co-methacrylic acid) macromolecules in aqueous solution: interplay between coulombic and hydrophobic interaction, Macromolecules 35 (2002) 1870–1876.

[46] Y. Bi, C. Yan, L. Shao, Y. Wang, Y. Ma, G. Tang, Well-defined thermoresponsive dendritic polyamide/poly(N-vinylcaprolactam) block copolymers, J. Polym. Sci. Part A: Polym. Chem. 51 (2013) 3240–3250.

[47] Y. Gao, S.C.F. Au-Yeung, C. Wu, Interaction between surfactant and poly(N-vinylcaprolactam) microgels, Macromolecules 32 (1999) 3674–3677.

[48] N. Häntzschel, F. Zhang, F. Eckert, A. Pich, M.A. Winnik, poly(N-vinylcaprolactam-co-glycidyl methacrylate) aqueous microgels labeled with fluorescent LaF3:Eu nanoparticles, Langmuir 23 (2007) 10793–10800.

[49] A. Laukkanen, S.K. Wiedmer, S. Varjo, M.-L. Riekkola, H. Tenhu, Stability and thermosensitive properties of various poly (N-vinylcaprolactam) microgels, Colloid Polym. Sci. 280 (2002) 65–70.

[50] T. Liu, J. Chen, S. Sugihara, Y. Maeda, Study on hydration of poly(N-vinylcaprolactam) microgels by near-IR and mid-IR spectroscopy, Colloid Polym. Sci. 290 (2012) 763–767.

[51] M.A. Moore, Theory of the polymer coil-globule transition, J. Phys. A: Math. Gen. 10 (1977) 305.

[52] X. Wang, X. Qiu, C. Wu, Comparison of the coil-to-globule and the globule-to-coil transitions of a single poly(N-isopropylacrylamide) homopolymer chain in water, Macromolecules 31 (1998) 2972–2976.

[53] H. Cheng, L. Shen, C. Wu, LLS and FTIR studies on the hysteresis in association and dissociation of poly(N-isopropylacrylamide) chains in water, Macromolecules 39 (2006) 2325–2329.